Supporting Information

Atomic-Layer-Deposited AZO Outperforms ITO in High-Efficiency Polymer Solar Cells

Zhipeng Kan,[1,2,+] Zhenwei Wang,[2,+] Yuliar Firdaus,[1,2] Maxime Babics,[1,2] Husam N. Alshareef,[1,] and Pierre M. Beaujuge[1,2,*]*

Physical Sciences and Engineering Division, [1]Materials Science & Engineering and [2]KAUST Solar Center, King Abdullah University of Science and Technology (KAUST), Thuwal 23955-6900, Saudi Arabia.

[+]co-first authors.

*To whom correspondence should be addressed. Email: pierre.beaujuge@kaust.edu.sa; husam.alshareef@kaust.edu.sa

Experimental section

AZO film deposition by ALD: The aluminum-doped zinc oxide (AZO) electrodes were deposited on glass substrates. The substrates were cleaned sequentially by acetone, isopropanol and de-ionized water using an ultrasonic cleaner (Branson 3510, Switzerland). The AZO films were then grown by atomic layer deposition (ALD) (system: Savannah 100, Ultratech). Further ALD deposition details are provided in the Supporting Information.

Material Characterizations: The thickness of the AZO films deposited by ALD was measured by profilometry (Dektak 8 Advanced Development Profiler, Veeco). The sheet resistance of the films was estimated from four-point conductivity measurements (CMT SR-2000 N, Advanced Instrument Technology; a correction factor of 4.46 was used during the measurements; distance between probes: 1 mm; sample size: 25.4 mm, square). The electrode work-functions were estimated by photoelectron spectroscopy in air (PESA) measurements (Model AC-2, Riken Keiki). The carrier density and Hall

mobility values were estimated by Hall effect measurements (Hall effect system 7607, LakeShore; sample size: 1×1 cm^2; sample connected to the Hall measurement system through van der Pauw-style connections from the four edges. UV-Vis transmittance spectra were acquired with a spectrophotometer equipped with an integrating sphere (Cary 6000, Varian). The X-ray diffraction (XRD) patterns of the AZO films were obtained with a Bruker D8 discovery X-ray diffractometer. Atomic force microscopy (AFM) measurements were performed with a scanning probe microscope operated in tapping mode (MFP-3D, Asylum Research). The AFM data was analyzed with the Gwyddion software. The chemical composition of the AZO films was analyzed by x-ray photoelectron spectroscopy (XPS) using an Axis Ultra DLD spectrometer (Kratos Analytical).

AZO electrode preparation: The AZO electrodes were patterned by wet etching, using diluted HCl as etching reagent (HCl:H_2O = 1.25:100 v/v). The AZO and ITO electrode areas and thicknesses were carefully measured by profilometry prior to the fabrication of PSC devices (**Figure S9**). The patterns were defined by photolithography (ECI 3027, MicroChemicals, Inc).

PSC device fabrications: The reference ITO-based PSC devices with the polymer donor PCE10 and the fullerene acceptor $PC_{71}BM$ (model systems) were prepared on ITO-patterned glass substrates (sheet resistance: 13 Ω sq^{-1}). The substrates were first scrubbed with dilute Extran 300 detergent solutions to remove organic residues, and were then immersed in an ultrasonic bath (Branson 5510) of dilute Extran 300 for 20 min. The samples were rinsed in flowing deionized water for 5 min before being sonicated for 10 min each in successive baths of acetone and isopropanol. Next, the samples were dried with pressurized nitrogen, and were then exposed to a UV-ozone plasma for 20 min. The ZnO precursor solution was prepared as reported in ref. 23 (ETL) was spin-cast at 3,000 rpm onto the ITO-patterned glass substrates, and the substrates were baked at 150°C for 15 min. Immediately after baking the substrates, the samples were then transferred into a dry nitrogen glovebox (< 3 ppm O_2) for active layer deposition.

The AZO-based PSC devices were prepared on glass substrates with patterned ALD-grown AZO (deposition: "20:1"AZO / 135 TMA cycles / 2700 DEZ cycles / substrate temperature: 200 ^oC / AZO thickness: 520 nm / sheet resistance: 16 Ohm/sq). The

substrates were rinsed in flowing deionized water for 5 min before being sonicated (Branson 5510) for 10 min each in successive baths of acetone and isopropanol. Note: The clean substrates were not subjected to any UV-ozone treatment. The solution-processed ZnO layer (ETL) was deposited following the same conditions described above for the reference ITO-based PSC devices.

The blend solutions of polymer donor (PCE10; purchased from One Material) and fullerene acceptor ($PC_{71}BM$; purchased from Nano C) were prepared in a nitrogen-filled glovebox. The polymer and fullerene counterparts were dissolved in chlorobenzene (CB), with 1,8 diiodooctane (3 vol%) being added as processing-additive, and the blend solutions were stirred for 12 hours at 70 °C. The active layers were spin-cast at room temperature from an optimum donor and acceptor blend ratios of 1:1.5 (wt/wt) and a solution concentration of 35 mg mL^{-1} (spin-speed: 2,500 rpm for 30 s; programmable spin-coater from Specialty Coating Systems (Model G3P-8)), resulting in films of *ca.* 100 nm in thickness. The samples were then allowed to dry at room temperature for 1 hour. Next, the samples were placed in a thermal evaporator for evaporation of a 7-nm layer of MoO_3 evaporated at 0.5 Å s^{-1} and a 120-nm layer of silver evaporated at 5 Å s^{-1}, at a pressure less than 1×10^{-7} Torr. Following electrode deposition, the samples underwent $J-V$ testing.

Thin film absorption: The UV-vis absorption spectra of PCE10 and $PC_{71}BM$ thin films on glass substrates were recorded with a Cary 6000i (Varian) UV-vis-NIR spectrophotometer equipped with an integrating sphere.

PSC device characterizations: The *J-V* measurements were performed in a nitrogen-filled glovebox equipped with a Keithley 2400 source meter and an Oriel Sol3A Class AAA solar simulator calibrated to 1 sun, AM1.5 G, with a KG-5 silicon reference cell certified by Newport. The external quantum efficiency (EQE) measurements were performed at zero bias by illuminating the device with monochromatic light supplied from a Xenon arc lamp in combination with a dual-grating monochromator. The number of photons incident on the sample was calculated for each wavelength by using a silicon photodiode calibrated by NIST.

The light intensity measurements were performed via PAIOS 2.1 instrumentation (Fluxim). PAIOS entails several device characterization techniques in steady-state and

transient modes. A first function generator controls the light source (a white LED – rise/fall time 100 ns); a second function generator controls the applied voltage. The current and the voltage of the solar cell devices are measured with a digitizer. The current is measured via the voltage drop over a 20 Ω resistor or a transimpedance amplifier, depending on the current amplitude. The white LED has 200 mW cm^{-2} of maximum power. Due to spectral mismatch, illumination from the white LED at 200 mW cm^{-2} does not provide 2 suns (AM 1.5G); 1 sun condition can however be reproduced by comparing the experimental J_{SC} and V_{OC} measured for the white LED-illuminated solar cells to the values obtained from AAA Solar Simulator illumination of the same device. During the measurements, the light intensity used ranged from 0.17 up to 1suns. When performing transient photocurrent measurements (see details below), the light pulses applied from the white LED source last for 200 μs using incident light intensity that ranged from 0.02 up to 1 suns as shown in **Figure S12**. When performing transient photovoltage measurements (see details below), the white LED source was used to produce both the perturbation light pulse and the background illumination light.

Transient photocurrent (TPC) analyses: TPC analyses measure the time-dependent extraction of photogenerated charge carriers. During the measurement, the PSC device is set under short-circuit condition; the devices are otherwise kept in the dark between pulses in order to avoid any influence of pulse frequency on the current responses.

Transient photovoltage (TPV) analyses: TPV analyses record the voltage decay of a device held at open-circuit upon continuous illumination, after a small perturbation light pulse has been applied. Note: TPC and TPV data were collected from averaging 150 measurements under each incident light intensity applied.

1. Additional information for AZO film deposition

The schematic ALD setup used for the AZO depositions is shown in **Figure S1a**. Commercial trimethyl aluminum (TMA, Sigma Aldrich product # 663301) and diethyl zinc (DEZ, Sigma Aldrich product # 668729) were used as the element precursors of Al and Zn, respectively. All precursors were used as received. Deionized water (DIW) was used as oxidant. Nitrogen (N_2) was used as carrier gas, the flow was set as 20 sccm during deposition. The base pressure was *ca.*

0.35 Torr during the deposition. The valves of the precursor cylinders were opened for a short time to provide the corresponding precursor pulses. The pulse/purge times (in seconds) for TMA, DEZ and DIW are 0.02/10, 0.015/10 and 0.015/10, respectively. During the deposition, all precursors were kept at room temperature. The temperature for the gas box and gas line were set as 150 ^{o}C, while the chamber temperature was set as 160, 200, or 250 ^{o}C during the optimization of the AZO film depositions. **Figure S1b** illustrates one cycle of the Zn-O (DEZ cycle) and Al-O (TMA cycle) sub-layer deposition, each sub-layer deposition contains one oxidant pulse (DIW) and one metal precursor pulse (DEZ or TMA). The AZO films were deposited by introducing one TMA cycle between several DEZ cycles; the Al content in the final AZO film can be tuned by changing the DEZ and TMA cycle ratio (DEZ/TMA ratio). **Table S1** shows the detailed TMA and DEZ deposition pulse sequence for the AZO films shown in **Figure 1a-c** (main text). The chamber temperature was set to 200 ^{o}C for this batch of AZO samples. All AZO films involved 900 DEZ cycles; the number of TMA cycles changed and depended on the DEZ/TMA ratio; the thickness for the AZO films was measured by reflectometry and the film thickness estimates are provided in **Table S1**. After optimizing the DEZ/TMA ratio, the deposition temperature of the AZO films was studied, while the DEZ/TMA ratio was kept at "20:1", and film thickness was controlled by setting the total number of DEZ cycles to 900. The deposition details are provided in **Table S2**. Finally, the optimization of the sheet resistance was achieved by varying the thickness of the AZO films via changes in the number of DEZ cycles from 900 to 2700. The deposition details for this batch of samples are shown in **Table S3**.

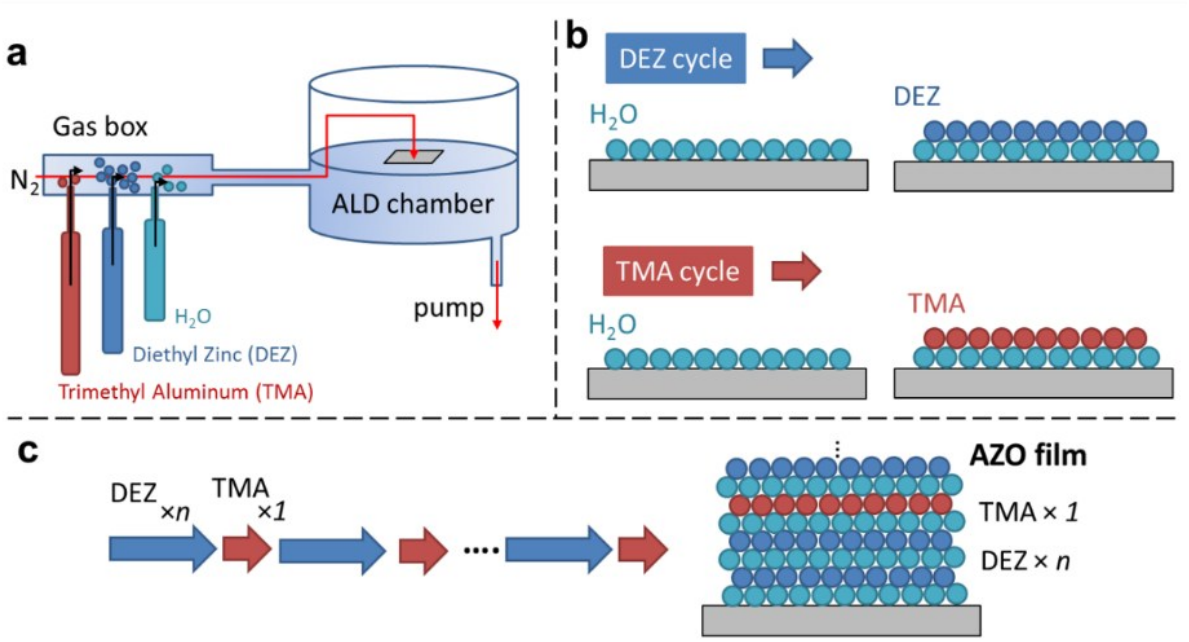

Figure S1 | Schematic of the ALD process and AZO film growth. (a) ALD setup for the depositions; (b) atomic schematic of the ALD DEZ and TMA precursor cycles: (c) illustration of the precursor pulse sequences employed to grow the AZO films by ALD.

Table S1 | Deposition details for ALD-grown AZO films with various DEZ/TMA ratios.

DEZ/TMA ratio	DEZ cycle	TMA cycle	Repeat times	Chamber temperature (°C)	Thickness (nm)
100:0	100	0	9	200	157.2
60:1	60	1	15	200	158.5
45:1	45	1	20	200	160.4
30:1	30	1	30	200	161.8
20:1	20	1	45	200	162.5
15:1	15	1	60	200	161.2
10:1	10	1	90	200	165.8
5:1	5	1	180	200	170.2

Table S2 | Deposition details for ALD-grown AZO films at various chamber temperatures.

DEZ/TMA	DEZ cycle	TMA cycle	Repeat times	Chamber	Thickness

ratio				temperature (°C)	(nm)
20:1	20	1	45	160	166.6
20:1	20	1	45	200	162.4
20:1	20	1	45	250	166.3

Table S3 | Deposition details for ALD-grown AZO films with various thicknesses.

DEZ/TMA ratio	DEZ cycle	TMA cycle	Repeat times	Chamber temperature (°C)	Thickness (nm)
20:1	20	1	45	200	162.5
20:1	20	1	90	200	338.2
20:1	20	1	135	200	517.8

2. Additional information for AZO film optimization

DEZ/TMA ratios series

The deposition details for the AZO films are shown in **Table S1**. The temperature during the ALD process was 200 °C and film thickness was controlled by setting the DEZ cycle number to 900. The photoelectron spectroscopy in air (PESA) spectra collected for the various ALD-grown AZO films are shown in **Figure S2**; the estimated work-function (Φ) values are shown in **Figure 1a**. The sheet resistance values were inferred from 4-point conductivity measurements (**Figure 1a**). The carrier concentration and Hall mobility data were obtained by Hall effect measurements (**Figure 1b**). The resistivity data pertaining to all AZO samples subjected to these two measurements is shown in **Figure S3**. The slight difference in resistivity observed from the 4-point and the Hall-effect measurements may come from the following two setup-related parameters: (i) measurement setup (linear 4 point for 4-point system; van der Pauw at 4 edge for Hall effect system), (ii) contact metal difference (Pt for 4-point system; In solder for Hall effect system). The UV-Vis transmittance spectra for AZO films grown at various DEZ/TMA ratios are shown in **Figure S4a**; the transmittance spectra cutting edge shifts to lower wavelength, indicating a widening of the optical bandgap. The tauc plots of these films are shown in **Figure**

S4b, and the extracted optical bandgap values (**Figure S4c**) confirm the bandgap increase upon Al doping.

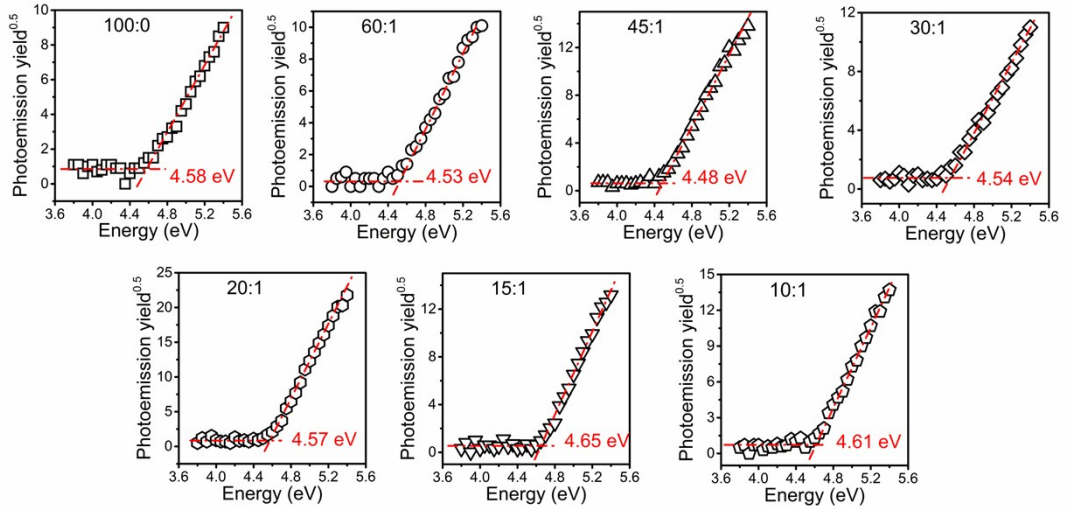

Figure S2 | Work-function analysis for AZO films grown from different precursor ratios; estimations obtained from photoelectron spectroscopy in air (PESA) measurements.

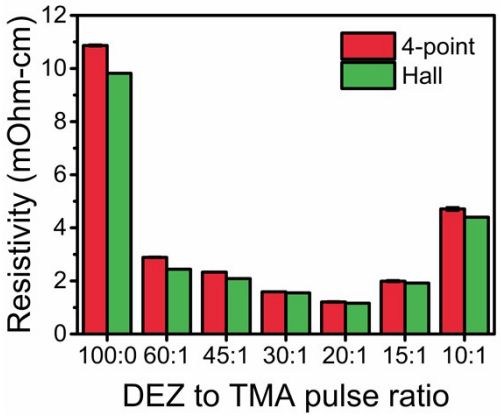

Figure S3 | Resistivity value of ALD-grown AZO films measured from the 4-point system and the Hall-effect measurement system.

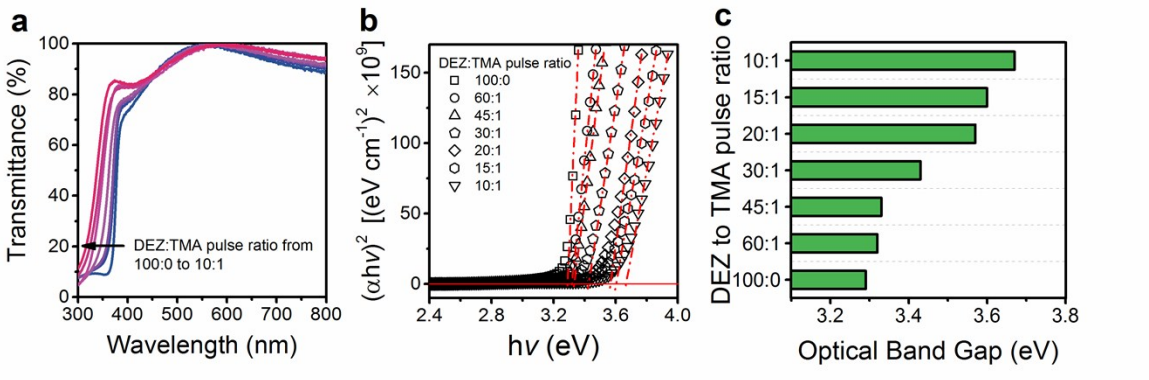

Figure S4 | Optical properties of AZO films grown from various precursor ratios. (a) UV-Vis transmittance spectra of AZO films; (b) corresponding tauc plot; (c) estimated optical bandgap determined from the tauc plots at each precursor ratio.

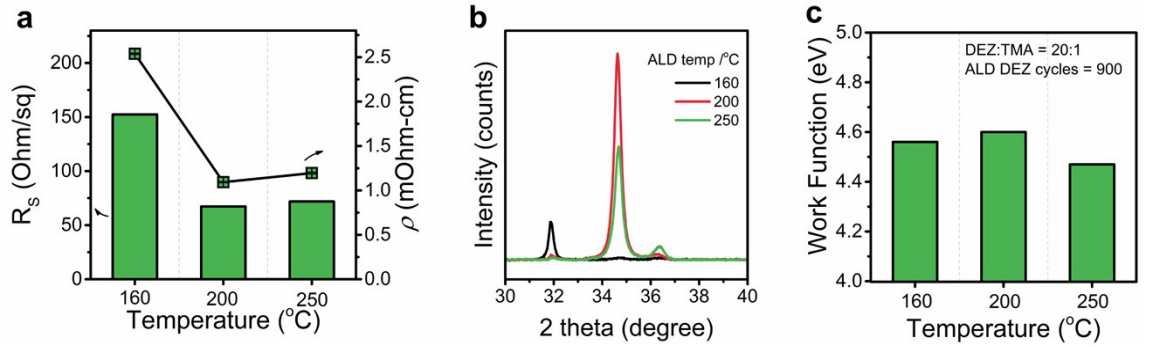

Figure S5 | Material properties of the "20:1" AZO films grown at different temperature. (a) Sheet resistance & resistivity; (b) XRD patterns; (c) work-functions.

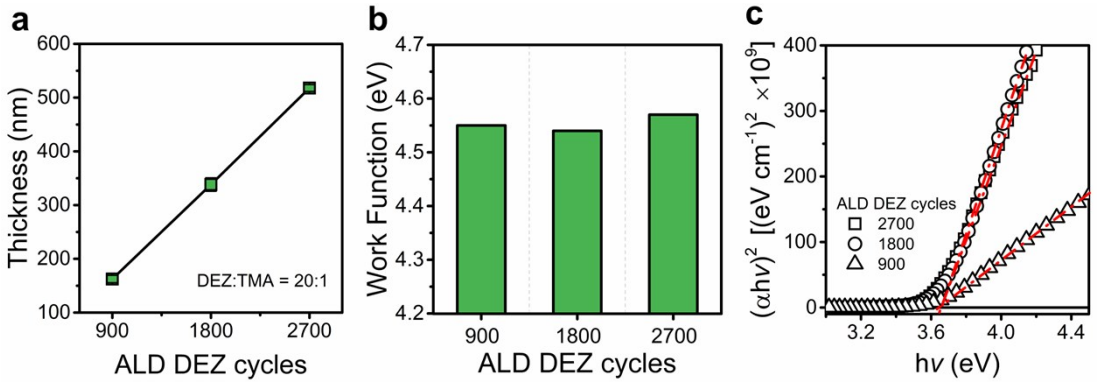

Figure S6 | Materials properties of the "20:1" AZO films. (a) Film thickness; (b) work-functions; (c) tauc plots for AZO films grown via 900, 1800 and 2700 DEZ cycles. The optical bandgap is indicated in the tauc plots.

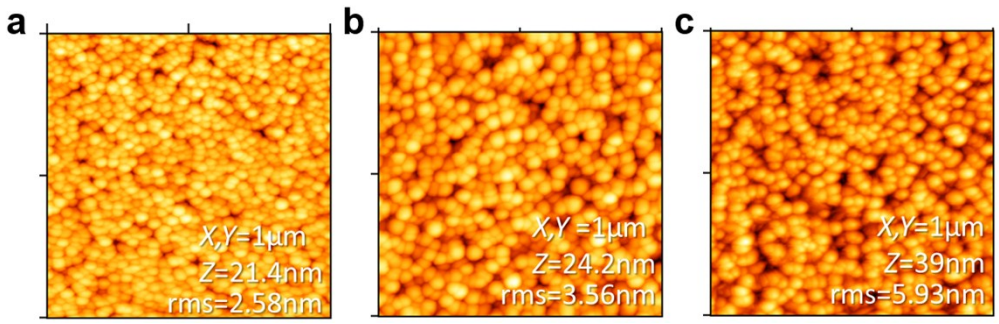

Figure S7 | AFM topography of AZO films grown with various DEZ cycles. (a) 900, (b) 1800, and (c) 2700 total DEZ cycles. The DEZ/TMA cycle ratio is "20:1", and the process temperature for ALD deposition is 200 °C.

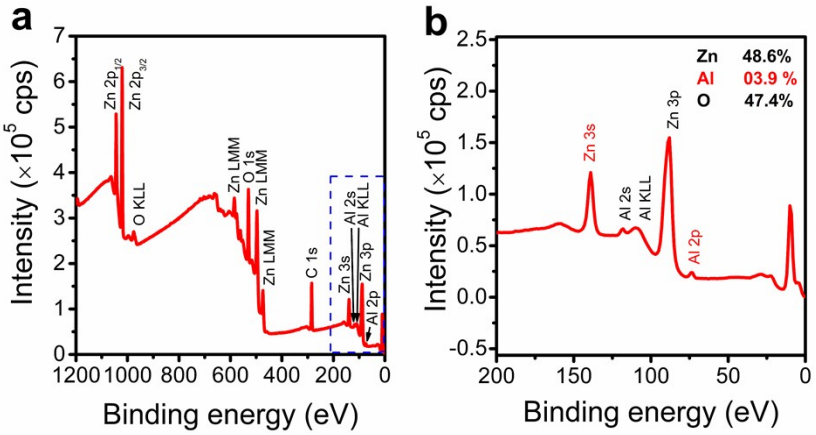

Figure S8 | XPS spectra of AZO films grown with 2700 DEZ cycles. The Al atomic content was calculated from the Al2p and Zn3s peak highlighted in (b).

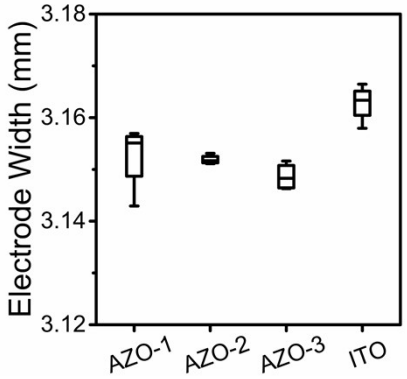

Figure S9 | ITO and AZO electrodes width determined by profilometry. AZO-1,2&3: AZO films grown with 900, 1800 & 2700 DEZ cycles.

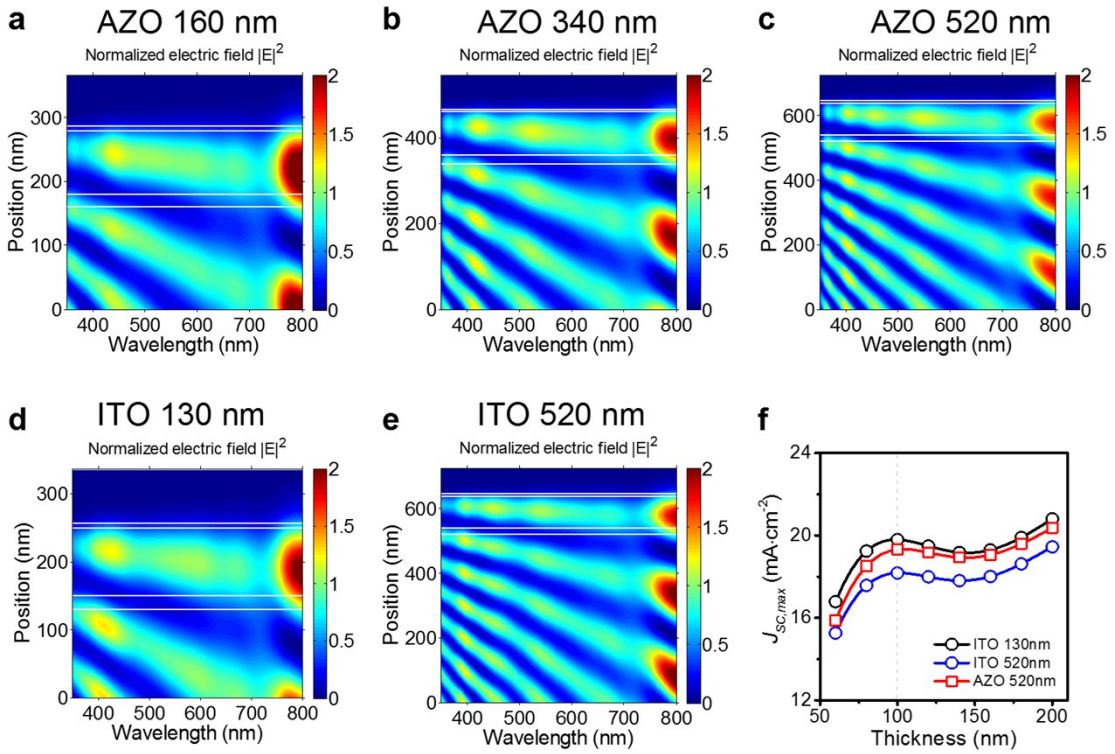

Figure S10 | Simulated optical field and J_{SC} of ITO- and AZO-based PSC devices. (a) – (e) simulated optical field of ITO- and AZO-based PSC devices with various electrode layer thicknesses; (f) simulated of ITO- and AZO-based devices as a function of active layer thickness.

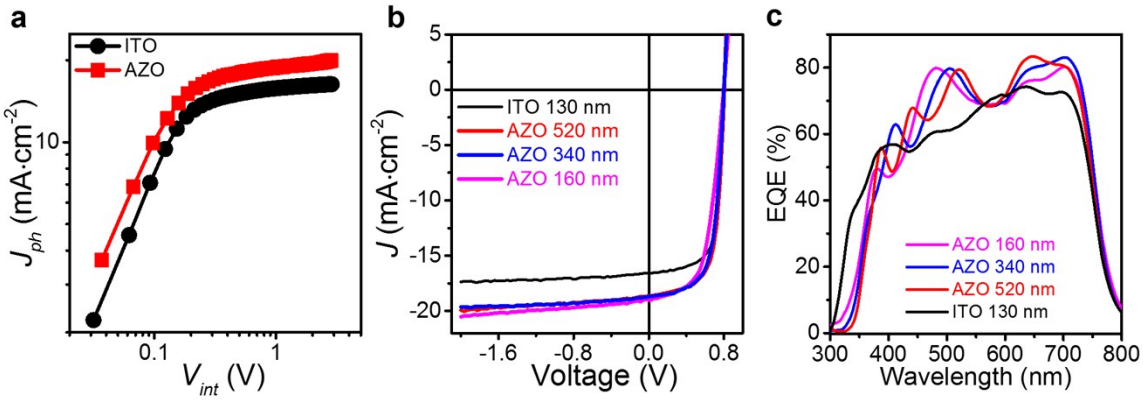

Figure S11 | Photocurrent as a function of effective voltage, *J-V*, and EQE characteristics of ITO- and AZO-base PSCs. (a) Photocurrent as a function of effective voltage; (b) *J-V*

characteristics of ITO- and AZO-based devices with various AZO film thicknesses; (c) EQE spectra of the corresponding films.

Table S4 | ITO- and AZO-based PSC device performance overview and statistics [a,b].

	V_{OC} (volt)	J_{SC} (mA cm^{-2})	FF (%)	PCE (%)	PCE (%) Max.
ITO 130nm	0.798±0.004	16.5±0.1	69.8±0.4	9.2±0.1	9.3
AZO 520nm	0.798±0.004	18.7±0.1	67.2±0.4	10.0±0.1	10.1
AZO 340nm	0.798±0.003	17.9±0.3	66.2±0.4	9.5±0.1	9.8
AZO 160nm	0.795±0.002	18.8±0.3	58.5±0.3	8.7±0.2	8.9

[a] Devices average values across 10 devices (device area: 0.1 cm^2). [b]Standard deviations calculated with the following equation (E1):

$$\sigma = \sqrt{\frac{1}{N}\sum_{i=1}^{N}(x_i - \mu)^2} \qquad \text{(E1)}$$

where σ is the standard deviation, μ is the arithmetic average value of the devices' PCE, N is the total number of devices used in the determination of the standard deviations.

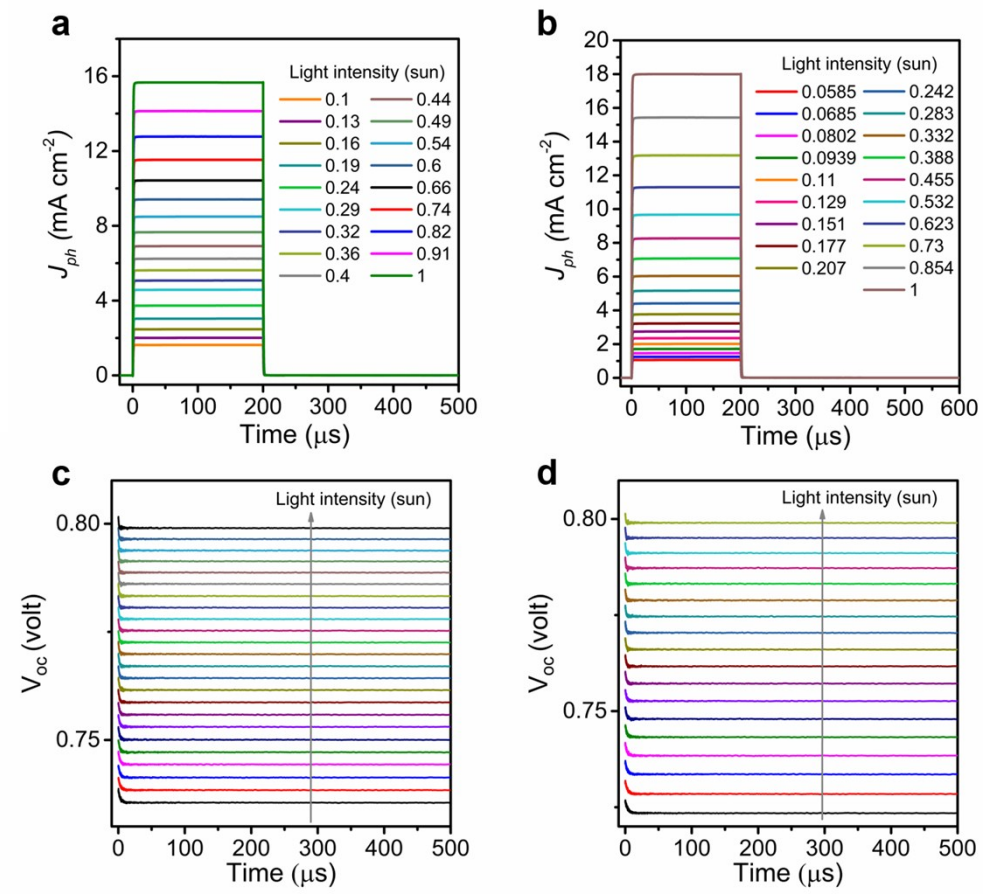

Figure S12 | Transient photocurrent and photovoltage. (a) TPC raw data of ITO-based device; (b) TPC raw data of AZO-based device; (c) TPV raw data of ITO-based device; (d) TPV raw data of AZO-based device.

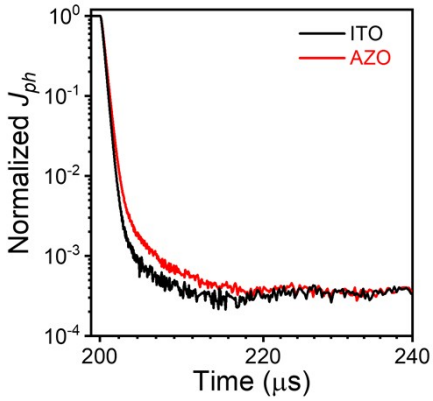

Figure S13 | Normalized Transient photocurrent. Normalized TPC data of ITO-based device, and AZO-based device; the TPC data were recoded under light intensity comparable to 1 sun.